Supervised Machine Learning and Feature Selection for a Document Analysis Application

James Pope[1] [a], Daniel Powers[1], J. A. (Jim) Connell[1], Milad Jasemi[1], David Taylor[2] and Xenofon Fafoutis[3]

[1]*Stephens College of Business, University of Montevallo, U.S.A.*
[2]*University of Memphis, U.S.A.*
[3]*DTU Compute, Technical University of Denmark, Denmark*

Keywords: Document Analysis, Supervised Machine Learning, Feature Selection, Optical Character Recognition.

Abstract: Over the past three decades large amounts of information have been converted to image formats from paper documents. Though in digital form, extracting the information, usually textual, from these documents requires complex image processing and optical character recognition techniques. The processing pipeline from the image to information typically includes an orientation correction task, document identification task, and text analysis task. When there are many document variants the tasks become difficult requiring complex sub-analysis for each variant and quickly exceeds human capability. In this work, we demonstrate a document analysis application with the orientation correction and document identification task carried out by supervised machine learning techniques for a large, international airline. The documents have been amassed over forty years with numerous variants and are mostly black and white, typically consist of text and lines, and some have extensive noise. Low level symbols are extracted from the raw images and separated into partitions. The partitions are used to generate statistical features which are then used to train the classifiers. We compare the classifiers for each task (e.g. decision tree, support vector machine, and random forest) to choose the most appropriate. We also perform feature selection to reduce the complexity of the document type classifiers. These parsimonious models result in comparable accuracy with 80% or fewer features.

1 INTRODUCTION

Automatically identifying text in images has enabled the extraction of knowledge from vast amounts of existing data. Optical Character Recognition (OCR) engines, trained for different languages, routinely recognise text in provided image files with remarkable accuracy (Ye and Doermann, 2015). However, these OCR engines typically assume the images to have low noise, correctly oriented, and minimal skew. Research continues to ensure the highest accuracy in extracting text from images, specifically in image preprocessing techniques.

In this paper we examine a specific text mining application for a large, international airline company that has amassed hundreds of thousands of maintenance work order documents since the 1980's. Internally the airline currently maintains electronic records, however, many maintenance tasks are carried out by various suppliers and original component manufacturers. There are efforts to standardise electronic exchange between airlines and suppliers, however, many still use physical documents to inform the airline of the maintenance performed on the component. These physical documents have been converted to electronic images using less than optimal scanners. Even as suppliers upgrade to electronic exchange, a vast amount of the maintenance history of the components in operational planes remains electronically inaccessible requiring tedious manual labour to acquire.

The airline's goal is to automatically extract as much information as possible from the work orders, where each work order consists of numerous documents. Correctly orienting and identifying the document's type are critical for achieving this goal. Figure 1 depicts the pipeline highlighting the document analysis process. Unfortunately there are numerous problems. Each scanned work order contains anywhere from 3-25 images. The images have noise, significant scan lines, and are arbitrarily oriented. Once

[a] https://orcid.org/0000-0003-2656-363X

Pope, J., Powers, D., Connell, J., Jasemi, M., Taylor, D. and Fafoutis, X.
Supervised Machine Learning and Feature Selection for a Document Analysis Application.
DOI: 10.5220/0008925104150424
In *Proceedings of the 9th International Conference on Pattern Recognition Applications and Methods (ICPRAM 2020)*, pages 415-424
ISBN: 978-989-758-397-1; ISSN: 2184-4313

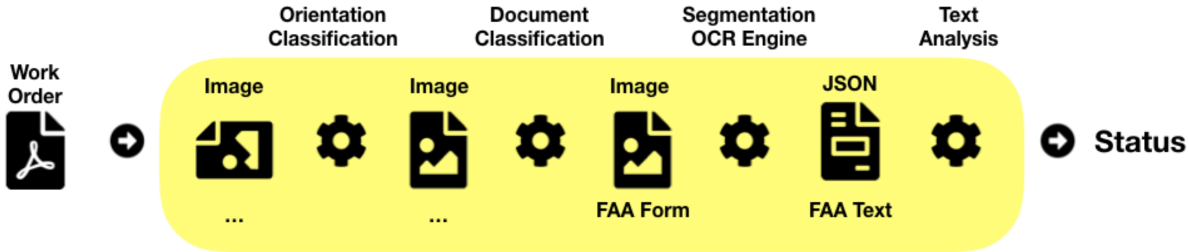

Figure 1: Document Analysis Process.

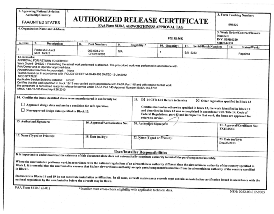

(a) north

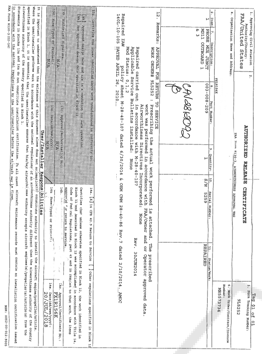

(b) east

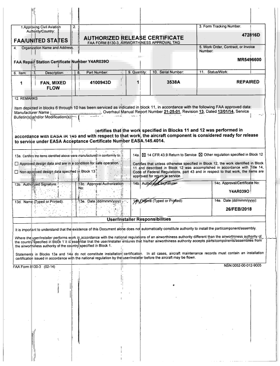

(c) north

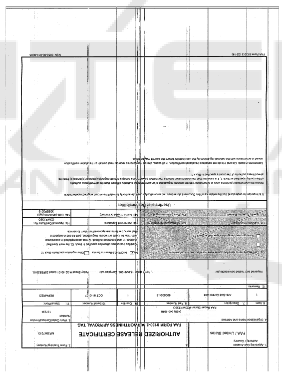

(d) south

Figure 2: Example Form Variants.

oriented and identified correctly, each document will require further processing including text area identification, optical character recognition, and text analysis. Considering the decades covered, there are numerous variants of each document. For example, we have identified at least 10 variants of one document of interest, the FAA Form 8130-3. Figure 2 shows four of these variants and their orientation. Note that (a) and (b) are wider than tall. Variants (c) and (d) also show significant scan line noise. These variants illustrate the difficultly in assuming any particular layout for automated processing. The problem is to automatically extract information from the work orders given these difficulties.

This paper examines our approach for obtaining information from these work orders using supervised machine learning techniques. We specifically focus on determining the status of the FAA Form, though the approach has been extended to other documents and information of interest. There are at least thirty identified document types. We use a sample of the work orders to train the classifiers by partitioning the images and calculating statistical measures for each partition from low-level symbols. Depending on the partition, there can be a large number of features generated. To reduce the complexity of the classifiers, we consider a shrinkage feature selection technique that considerably reduces the number of features while maintaining comparable accuracy. The contributions of this paper are enumerated as follows:

- Practical approach to orientation and document classification using only symbol features without resorting to an OCR engine.
- Comparison of machine learning algorithms for these symbol features.
- Application of machine learning and feature selection for document analysis.

We further stipulate that our approach makes no assumptions regarding the font type and font size. The rest of the paper is organised as follows. The related work is discussed followed by the feature extraction process. The orientation and document classifiers are presented along with their results and analysis. Next the text analysis and end-to-end results are presented followed by the conclusion.

2 RELATED WORK

Lu and Tan (Lu and Tan, 2006) propose converting the documents into vectors using language information, density, and vertical components. Training vectors are then compared against for orientation detection and document classification. Rangoni, et al. (Rangoni et al., 2009), propose a method that does not depend on the specific text symbols used to infer the orientation. Instead it uses the OCR engine and selected text

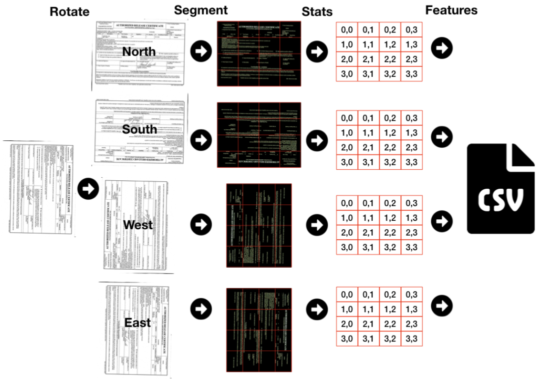

Figure 3: Feature Extraction Task.

to determine the orientation. Yang, et al. (Yang et al., 2017), focus on text recognition from biomedical literature. They propose a system that performs multi-orientation text detection, cropped word and end-to-end recognition. Their approach does not explicitly model the orientation of the document.

O'Gorman (O'Gorman, 1993) proposed a bottom-up, nearest neighbour clustering approach for page layout analysis. This has been a popular technique for page layout analysis with many variants and heuristics added. Ye, et al. (Ye and Doermann, 2015), survey existing techniques and problems for text recognition in images highlighting the multiple orientation issue.

Research in model selection continues and can roughly be categorised as subset selection, shrinkage methods, and dimension reduction techniques (James et al., 2014). The Forward Stepwise subset selection starts with no features in the model and adds them one at a time. It can be evaluated using estimates of the test error (e.g. AIC, BIC, adjusted R^2) or directly using a validation set or cross-validation. LASSO (Tibshirani, 1994) and Elastic Net (Zou and Hastie, 2005) are shrinkage techniques. LASSO adds an $L1$ norm penalty of the coefficient vector to the residual sum of squares. This norm is multiplied by the weighting parameter λ. This can also be evaluated using cross-validation.

3 FEATURE EXTRACTION

This section details how the image is processed from a raw pixel representation to an annotated instance with several hundred features. We use the notation N to represent the number of training instances and D to represent the number of features (i.e. dimensions). Each work order typically consists of between four to eight documents stored as images in a PDF. For this

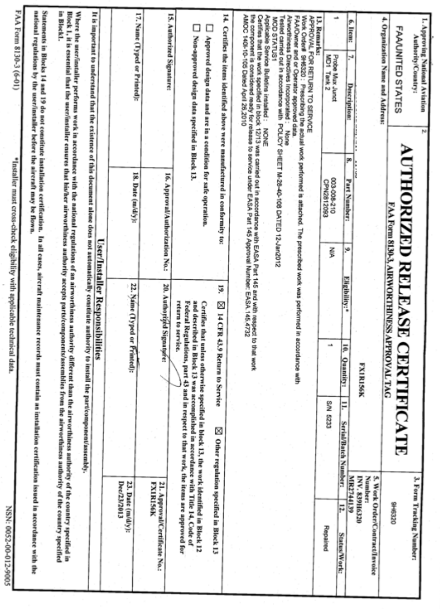

Figure 4: Original Image.

work, we assume that the images have been extracted and make the following assumptions:

- Images are scanned from form style documents (also referred to as tabular documents) primarily consisting of text and lines.
- Images consist mostly of black and white pixels or can easily be converted (e.g. grey scale images).
- Most of the text symbols in the image are separable - i.e. non-cursive.
- Most of the text symbols are similarly aligned; we do not assume mixed aligned text.

The following section details how pixels are converted into symbols. The subsequent sections detail how the symbol attributes are used to generate the features for each image.

3.1 Symbol Extraction

The FAA Form 8130-3 contains black text, lines, and figures with a white pixel background. Figure 4 shows an example of the form. Most of the pixels are either black (0,0,0) or white (255,255,255). Given the form image, the file is read in and inverted to a pure black background with pure white text, lines, and figures. A connected components algorithm is then run on the image to group all pixels that are connected into a *symbol*. We found that using a weighted union-find with path compression (Sedgewick and Wayne, 2011) performs well for determining the connected components and is scalable with a time complexity near linear in the number of pixels.

Table 1: Performance Metrics per Document Image.

Metric	Value
Mean Time to Partition	0.8107 second
Mean Number of Pixels	8498281
Mean Number of Total Symbols	13226
Mean Number of Symbols Filtered	10986

To eliminate noise, we filter the symbols by number of points. Symbols with less than ~ 20 points are believed to be noise or uninteresting symbols (another common approach would be to use a Gaussian filter / threshold).

The remaining symbols are then augmented with information about their neighbours. The K nearest neighbours are determined using the distance between the centroids of the symbols. The approach is performed using a kD-tree to help avoid brute-force calculation against all neighbours.

To demonstrate the efficiency of the approach, we ran the process on 452 images (from 113 original documents rotated in the four orientations) and collected metrics. The experiments were conducted ten times on a standard MacBook Pro laptop (2.6 GHz Intel Core i7). Table 1 shows the results. It takes less than one second to produce the features for an image. It is interesting to note the number of filtered noise symbols (10986). This is due to the shaded regions on many of the images (see Figure 2 (b) and (d)). Each symbol has the following attributes.

- Number of black pixels
- Number of white pixels
- Density, white pixels / black pixels
- Bounding box pixel width and height
- Aspect ratio (width / height)
- Neighbour vector (distance and angle between centroids)

3.2 Symbol Feature Generation

After each image is processed from raw pixels into a set of symbols, the symbols are partitioned based on the their centroid. The partition bounds are rectangular based on the number of columns and rows specified. For example, if 4 rows and 4 columns are specified for an image that is 2000 x 3000 pixels, the partitions are 500 x 750 pixels. For this work we assume the number of rows and columns to be the same which we denote as P. Thus the number of partitions is P^2. Note that some symbol area may extend into adjacent partitions - the symbol is placed into the partition that contains its centroid point. Figure 5 shows

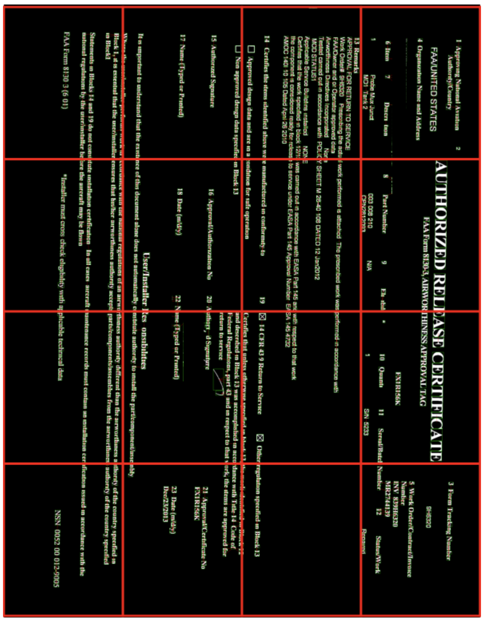

Figure 5: Partition $P = 4$.

the result of the partition of the form shown in Figure 4.

The number of points, neighbour angles, and density for the symbols are heavily skewed. For this reason we choose to use the median as a central tendency measure for each partition. For each partition the following features are recorded.

- Number of symbols in the partition
- Median neighbour angles
- Median aspect ratio
- Median symbol density
- Partition Density

As P increases there will be more and more partitions that have no symbols. For this, we record 0 for the number of symbols and 0 for the partition density and leave the aspect ratio, neighbour angle, and symbol density as missing values.

3.3 Aspect Ratio

The aspect ratio is defined as the width / height for each symbol. For each partition, we take the median aspect ratio. For these particular documents we find that a ratio below approximately 0.95 is indicative of north or south orientation and above 0.95 is indicative of east or west orientation.

3.4 Symbol Neighbour Angle Calculation

The centroid of each symbol is denoted as vector **u** and a neighbour's centroid is denoted as vector **v**. Note that we first have to translate **v** to **u** by subtracting to produce a new vector $\mathbf{a} = \mathbf{v} - \mathbf{u}$. We normalise **a** and compute the dot product with a unit vector **b** pointing east (1,0). Because both vectors are unit, we can simply determine the $cos(\theta) = \mathbf{a} \cdot \mathbf{b}$, where θ is the angle between the vectors. For the rest of the paper we consider this $cos(\theta)$ synonymous with neighbour angle.

We do not need the actual angle in degrees and simply use $cos(\theta)$ as the feature. We take the absolute value to get values between $[0.0, 1.0]$, where values near 0.0 indicate the neighbour is to the west or east from the symbol and values near 1.0 indicate the neighbour is to the north or south.

3.5 Number of Neighbours K

The number of neighbours for the expected neighbour angle was also considered and is used in other problem domains. O'Gorman suggests using $K = 5$ for extracting text blocks (O'Gorman, 1993). Figure 6 shows the result for $K = 1$. Each symbol is surrounded by a green bounding box and red lines are drawn to each neighbour. We empirically found that it was sufficient to only consider $K = 1$ for orientation detection (results omitted for brevity).

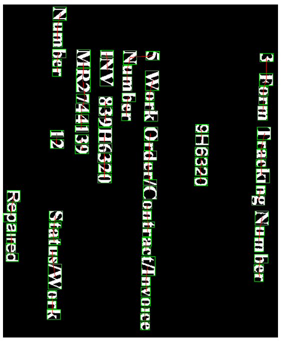

Figure 6: $K = 1$ Nearest Neighbours.

3.6 Number of Symbols

The number of symbols is also available for each partition. Interestingly, Figures 11 and 10 show that the number of symbols are critical for determining the document's type.

3.7 Document Features

In addition to the features for each partition, we calculate the following features for each document.

- Document width
- Document height
- Document number of symbols
- Document median density
- Aspect ratio (width / height)
- Document median neighbour angle
- Orientation
- Document order in the PDF

Figure 7 shows the segment density versus neighbour angle. Similar to the aspect ratio, this feature is very good at separating north and south from east and west orientations. Figure 8 shows it being used as the root, though a better split value would have been 0.5 rather than the selected 0.119145.

It should be noted that there will be some correlation between these document features and partition features (e.g. the number of document symbols will be related to the number of symbols in the partitions). The total number of features D for each document is given by the following formula.

$$D \ \#features/document = (P^2 \times 5) + 8 \qquad (1)$$

For example, a $P = 4$ partition results in $D = 88$ features for each image. We repeat this for each image and save as a comma-separated values (CSV) file. This file is then manually annotated to include the correct orientation and document type. We designate the orientation as one of $\{east, north, west, south\}$ (0, 90, 180, 270 degrees respectively). There are approximately thirty different document types. In this paper we simplify and only consider the two classes $\{faa, other\}$. We next analyse the orientation and document type classifiers built using these features. We use decision trees to assist in the analysis because they are relatively easy to interpret.

4 ORIENTATION CLASSIFICATION

We evaluate how well the features can be used to infer the orientation and the effect that P has on the various classifiers. A failed orientation detection very likely results in a failed optical character recognition, thus we consider false positives and false negatives

Table 2: Classifier Settings.

Classifier	Settings
Naive Bayes	NA
Decision Tree	-C 0.25 -M 2
Support Vector Machine	-C 1.0 -K PolyKernel
Random forest	-P 100
Logistic Regression	-R $1e10^{-8}$ -M -1

to be equal in cost. Considering this and since each class is balanced we choose to use the accuracy measure to compare the various experiments. We use the Weka data mining software (Hall et al., 2009) (version 3.9.3, 2019) to analyse the data. For the remainder of this paper we use the classifiers listed in Table 2 using the typical settings for this library. In several figures we use the notation $c0r4\_segmentDensity$ to indicate a specific feature for a partition (e.g. segment density for partition column 0 and row 4). If the partition is omitted it should be assumed to be a document feature. A brief analysis of the features with respect to orientation is first presented followed by a comparison of the accuracy of various classifiers using the generated features.

4.1 Orientation Classifier Analysis

We consider the partition $P = 5$ with 133 features. Examining the scatter plots of the features against each other it was clear that the document median angle and certain partition segment densities provide useful information regarding orientation. Figure 7 shows a plot of the median angle (x-axis) versus partition c4r4's segment density. For illustration some jitter has been added to distinguish the points.

The figure's results are somewhat expected. For English text the nearest symbol would be to the left or right when oriented north or south. Conversely when oriented east or west the nearest neighbour would be above or below the symbol. Interestingly, the figure also shows that the selected partition's segment density can be used to distinguish between the north and south orientation.

Figure 8 shows the corresponding decision tree. We restricted the size of the tree for illustration purposes (required leaf nodes to have a minimum of 100 instances).

The decision tree classifier takes advantage of the document median angles and splits at 0.83 (though 0.5 would appear to suffice as well). As Figure 7 shows most north-south orientation instances are nearer to 1.0 and east-west are nearer to 0.0. The right half of the tree then uses the partition's segment density to differentiate north from south. The classifier uses another partition segment density to differentiate east from west. The document median angle and specific partition segment densities are important for orientation classification. We also found that the document median aspect was also able to distinguish north-south from east-west similar to the document median angle. This is also reasonable as we would expect English text height to be more than the width on the average.

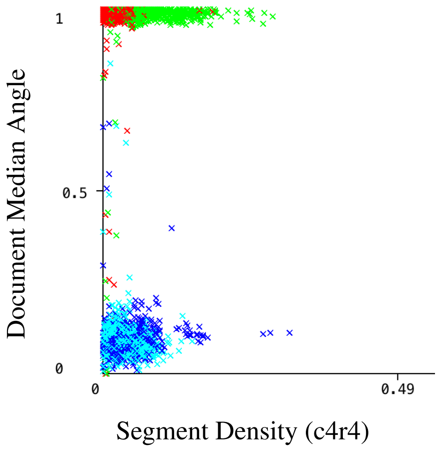

Figure 7: Orientation Scatter Plot $P = 5$. Legend: north south east west.

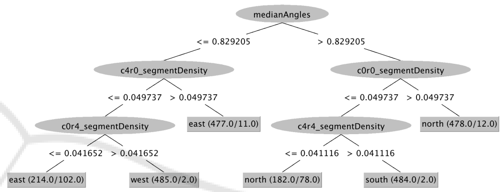

Figure 8: Orientation Decision Tree $P = 5$.

Table 3 shows the confusion matrix for the decision tree classifier (with the node size restriction removed) trained using 10 fold cross validation. We would expect there to be errors between east and west and north and south. We would not expect a north, south orientation to be confused as east,west and visa versa. The results confirm this as most errors occur between north vs south and east vs west.

Table 3: Decision Tree Confusion Matrix $P = 5$.

Accuracy=0.972		Predicted			
		east	*north*	*south*	*west*
Actual	*east*	563	0	1	16
	north	1	565	14	0
	south	1	16	563	0
	west	15	0	1	564

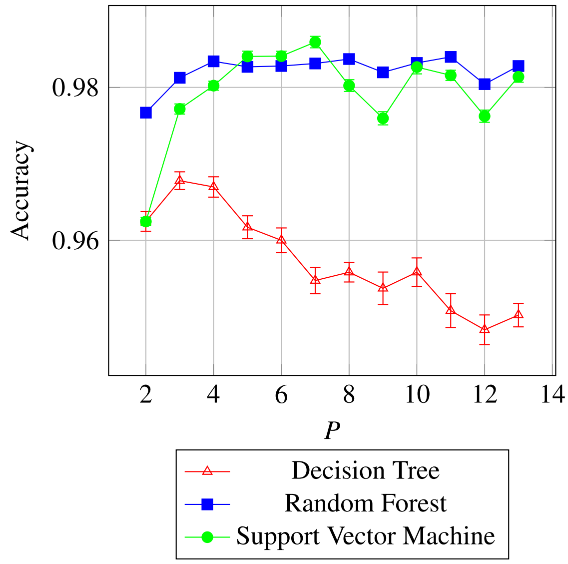

Figure 9: Orientation Accuracy 10-Fold Cross Validation.

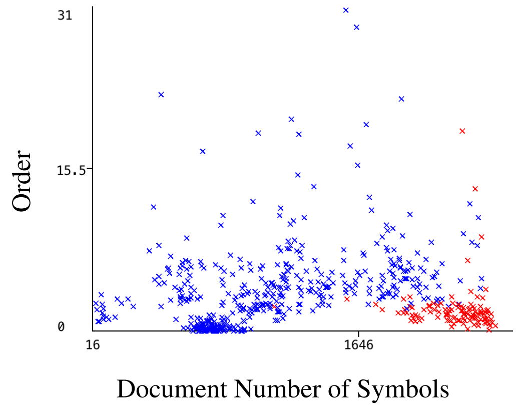

Figure 10: Document Type Scatter Plot $P = 5$. Legend: {other, faa}.

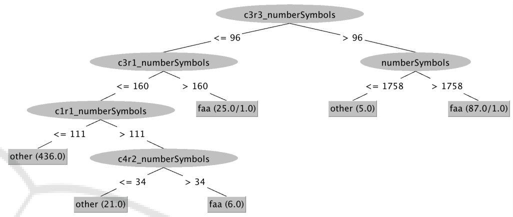

Figure 11: Document Type Decision Tree $P = 5$.

4.2 Orientation Classifier Accuracy

We use the annotated files for each value of P from 2 to 13 with $N = 2320$ instances to train several orientation classifiers. Due to limited training instances, we train each classifier on the file using 10 fold cross validation. We run this 30 times for each classifier and take the average of the accuracy to produce Figure 9 with 99% confidence intervals. The results are shown 9. When $P = 2$ most classifiers perform poorly. We believe this is because too much aggregation has occurred and obscured differentiating information. As P increases, the reason we believe the decision tree performs poorly is because this creates more and more irrelevant and correlated features. This has a negative effect on some classifiers including decision trees and naive Bayes (specifically correlated features) whereas other classifiers, such as support vector machines, are less impacted by these issues (Tan et al., 2019).

The ensemble random forest classifier appears to do quite well for all values of P including $P = 2$. The random forest and support vector machine do well between $3 =< P <= 6$ achieving near 98% accuracy. The random forest's accuracy across all values of P make it a strong candidate.

5 DOCUMENT CLASSIFICATION

Similar to the orientation classifier, we evaluate how well the features can be used to infer the document type and the effect that P has on the various classifiers. We assume the orientation has been determined and therefore only consider each image in its north orientation with $N = 580$ annotated instances. We first consider a brief analysis of the features and then consider a comparison of the accuracy of various classifiers.

5.1 Document Type Classifier Analysis

Similar to the orientation classifier, we examine the partition $P = 5$ with 133 features. Figure 10 shows a plot of the document's number of symbols (x-axis) versus the document's order (with some jitter added). A relatively simple selection statement would do well considering documents with more than 1800 symbols and an order with 2 or 3. Figure 11 shows the corresponding decision tree.

Interestingly, as Figure 11 shows, the decision tree classifier primarily relies on the number of symbols features. Other partition sizes do use the order. However, we also found the document median density feature to be just as effective as the order. We determined this by removing the order feature and were able to obtain similar accuracy results. Note that we did not restrict the size of the tree. These results provide evidence that many feature are either redundant (i.e. correlated with other features) or superfluous for document type classification. Section 7 will provide more evidence for this assertion. Table 4 shows the confusion matrix for the decision tree. To remain consistent, the classifier was trained using 10 fold cross vali-

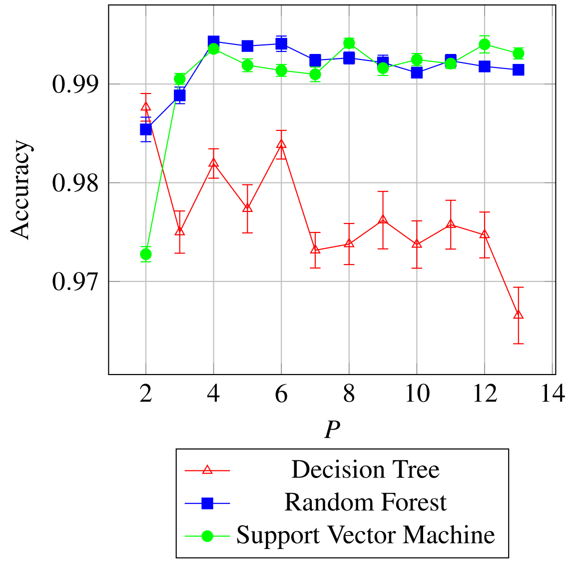

Figure 12: Document Accuracy 10-Fold Cross Validation.

dation. We do note that for highly imbalanced classes the number of folds may need to be adjusted (Raeder et al., 2012). There are roughly the same number of false positives as false negatives.

Table 4: Decision Tree Confusion Matrix $P = 5$.

Accuracy=0.9776		Predicted	
		other	*faa*
Actual	*other*	457	7
	faa	6	110

5.2 Document Type Classifier Accuracy

We again choose to use the accuracy measure to compare the various experiments and use similar settings shown in Table 2. We train each document type classifier using 10 fold cross validation and run this 30 times for each classifier and compute 99% confidence intervals.

Figure 12 shows the results of the experiments. For $P = 2$ the decision tree and random forest perform notably better than the support vector machine. From $P = 2$ to $P = 3$ the situation reverses and the decision tree performs progressively worse, as was the case with the orientation classifier. After $P = 3$ the random forest and support vector machine produce similar results around 99% accuracy.

6 OCR AND TEXT ANALYSIS

Once images have been oriented and the document identified, selected images are segmented and sent to the optical character recognition (OCR) engine. After a qualitative comparison of several tools, it was decided to use Tesseract (Kay, 2007) as the OCR engine in the pipeline. The north oriented FAA form image is segmented to form a set of symbols. The symbols are combined to form a suspected line of text (termed *document streams* (O'Gorman, 1993)). Neighbouring symbols are combined if within some angle to the left and right and within some distance, both empirically determined. Once the document streams have been OCR'ed the produced text stream, (x, y) coordinates, and bounding box are written to a Javascript Object Notation (JSON) file.

The final text analysis step in Figure 1 performs the following relatively simple procedure. The text streams are filtered to only examine those in the area of interest (in this case, the upper right quadrant). Then each text stream is checked against a small set of predetermined words. The Levenstein distance is taken and the shortest distance is taken to the intended word. Though simple this final step can also handle false positive document classifications (images that are not FAA forms but were identified as such and OCR'ed). Of course, more extensive text analysis can be performed and reinforce document classification (e.g. using a bag of words approach). The text analysis classifies as one of the following status' $\{$*repaired*,*tested*,*inspected*,*overhauled*,*other*$\}$.

7 FEATURE SELECTION

We used the shrinkage method LASSO to select a subset of the features for the document type classifier. We compare the accuracy of the LASSO classifiers to the full model classifiers. We do not necessarily expect the LASSO classifiers to have a higher accuracy but would prefer that they are not significantly lower. First the training set features for each partition size are standardised ($\bar{x} = 0.0, \sigma = 1.0$). Missing values are then set to the mean of 0.0. We then used the *glmnet* (Friedman et al., 2010) R package for the analysis and figure generation. To evaluate the models we selected cross-validation. With x representing all the standardised features and y the response variable **type**, we used the following command *cv.glmnet(x,y, family = "binomial")*.

Figure 13 shows the log of λ versus the *deviance* for a 10-fold cross validation to determine a suitable value for λ for the $P = 5$ partition. The deviance is an analogous measure to residual sum of squares but for more general models and is negative two times the maximised log-likelihood (lower is a better) (James et al., 2014). For each value of λ the upper and lower

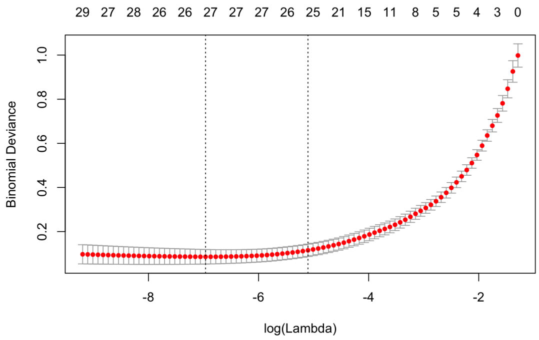

Figure 13: Binomial Deviance λ.

standard deviation is also shown. The first dashed vertical line represents the λ^* that resulted in the lowest deviance. Because we prefer a model with fewer features we use the common heuristic of selecting the matching λ to the right of λ^*'s upper standard deviation. This is within one standard deviation of λ^* and has fewer features (from roughly 27 to 25). This is shown as the second dashed vertical line. Overall, this went from 133 features (per Equation 1) to just 25, a reduction of $\tilde{8}0\%$.

This process is repeated for each partition size from $P = 2$ to $P = 14$ where a subset of features are selected from the total set of features. Figure 14 shows the total number of features versus the number of features chosen by LASSO. The number of features for LASSO rises slightly from $P = 2$ to $P = 5$. However, after approximately $P = 5$ the number of features selected by LASSO appears to stop increasing (the values never exceed 34 features). At $P = 4$, the number of features for the LASSO model is 15 versus 88 for the full model, a ratio of $\sim$17%. At $P = 14$, the number of features for the LASSO model is 28 versus 988 for the full model. The ratio between the number of features for the LASSO model and the full model is never more than 80% when $P = 5$. We believe this is expected. At some point increasing the number of features would not help the model as the partitions become smaller and smaller and no significant aggregation is obtained.

The document number of symbols and document order from Section 3.7 appear in all LASSO models except for one indicating their importance. The FAA document typically appears second or third in the order suggesting some ordering procedure in the scanning process. The document median density also appears in more than half the models. The median document density is likely correlated with the document number of symbols. A drawback of LASSO is that it arbitrarily selects one of a set of correlated features.

For the same models shown in Figure 14, using the support vector machine classifier, we compute their

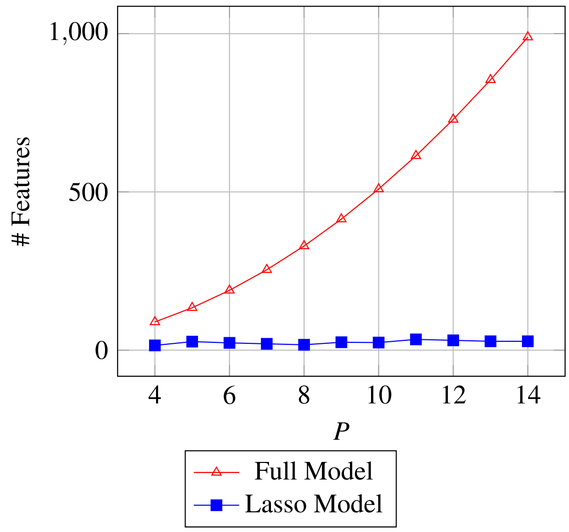

Figure 14: Features: Full Model vs LASSO Model.

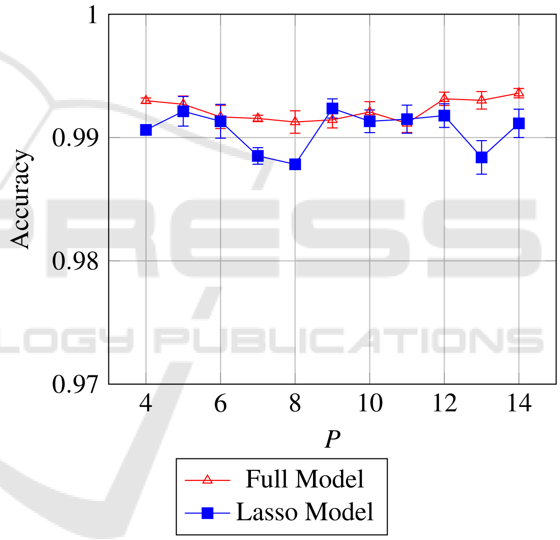

Figure 15: Document Accuracy Full vs LASSO Model.

accuracy results 30 times and plot them in Figure 15 with 99% confidence intervals. The accuracy results of the LASSO model are comparable to the full model or indistinguishable.

8 STATUS CLASSIFICATION RESULTS

To demonstrate the overall efficacy of our approach, we consider the classification of the FAA status as shown in Figure 1 for each work order. A correct classification requires the orientation, document type, document stream identification, optical character recognition, and text analysis to also be successful.

To be clear, this is not an ideal validation. Though we have been using cross validation approaches throughout, a significant test set would be more convincing (future work is to obtain this).

The pipeline was run on the 116 work orders with 1106 images where 117 are FAA documents (one work order had a duplicate FAA form). All 117 FAA documents were correctly oriented. The document type classifier predicted 121 documents to be FAA where four were false positives (non-FAA images classified as FAA). The text classifier predicted three of the four as *other* and one as *tested* (i.e. it mitigated three of four false positives). The text classifier correctly predicted the status of 116 FAA documents with one incorrectly predicted as *tested* versus actual *repaired*.

9 CONCLUSIONS

In this paper we proposed and demonstrated an approach for document analysis using a combination of supervised machine learning models for orientation classification and document classification. The form style documents were first partitioned to produce symbols from which features were generated. The features were then used to train machine learning algorithms. When the image is oriented and the document identified, document streams are sent to an OCR engine to produce a text file from which a simple match is made to determine the desired form's status. We then employed a feature selection approach for the document type classifier to produce a parsimonious model and showed that it was as accurate as the full model. Finally, the end-to-end results were presented to demonstrate the effectiveness of our approach.

ACKNOWLEDGEMENTS

This work was supported in part by the University of Montevallo Contract #19-0501-001. The authors greatly appreciate the support of the airline company employees involved in the project. Without their efforts this research could not have been conducted.

REFERENCES

Friedman, J., Hastie, T., and Tibshirani, R. (2010). Regularization paths for generalized linear models via coordinate descent. *Journal of Statistical Software*, 33(1):1–22.

Hall, M., Frank, E., Holmes, G., Pfahringer, B., Reutemann, P., and Witten, I. H. (2009). The WEKA Data Mining Software: An Update. *SIGKDD Explor. Newsl.*, 11(1):10–18.

James, G., Witten, D., Hastie, T., and Tibshirani, R. (2014). *An Introduction to Statistical Learning: With Applications in R*. Springer Publishing Company, Incorporated.

Kay, A. (2007). Tesseract: An open-source optical character recognition engine. *Linux J.*, 2007(159):2–.

Lu, S. and Tan, C. L. (2006). Automatic document orientation detection and categorization through document vectorization. In *Proceedings of the 14th ACM International Conference on Multimedia*, MM '06, pages 113–116, New York, NY, USA. ACM.

O'Gorman, L. (1993). The document spectrum for page layout analysis. *IEEE Transactions on Pattern Analysis and Machine Intelligence*, 15(11):1162–1173.

Raeder, T., Forman, G., and Chawla, N. V. (2012). *Learning from Imbalanced Data: Evaluation Matters*, pages 315–331. Springer Berlin Heidelberg, Berlin, Heidelberg.

Rangoni, Y., Shafait, F., Van Beusekom, J., and Breuel, T. M. (2009). Recognition driven page orientation detection. In *Proceedings of the 16th IEEE International Conference on Image Processing*, ICIP'09, pages 1969–1972, Piscataway, NJ, USA. IEEE Press.

Sedgewick, R. and Wayne, K. (2011). *Algorithms, 4th Edition*. Addison-Wesley.

Tan, P., Steinbach, M., Karpatne, A., and Kumar, V. (2019). *Introduction to Data Mining, Second Edition*. Pearson.

Tibshirani, R. (1994). Regression shrinkage and selection via the lasso. *JOURNAL OF THE ROYAL STATISTICAL SOCIETY, SERIES B*, 58:267–288.

Yang, C., Yin, X., Yu, H., Karatzas, D., and Cao, Y. (2017). ICDAR2017 robust reading challenge on text extraction from biomedical literature figures (DeTEXT). In *2017 14th IAPR International Conference on Document Analysis and Recognition (ICDAR)*, volume 01, pages 1444–1447.

Ye, Q. and Doermann, D. (2015). Text detection and recognition in imagery: A survey. *IEEE Transactions on Pattern Analysis and Machine Intelligence*, 37(7):1480–1500.

Zou, H. and Hastie, T. (2005). Regularization and variable selection via the elastic net. *Journal of the Royal Statistical Society, Series B*, 67:301–320.